Conformational Studies of d-(AAAAATTTTT)$_2$ Using Constraints from Nuclear Overhauser Effects and from Quantitative Analysis of the Cross-Peak Fine Structures in Two-Dimensional ^{1}H Nuclear Magnetic Resonance Spectra†

Bernardo Celda,‡,§ Hans Widmer,‡ Werner Leupin,‡,∥,# Walter J. Chazin,‡,⊥ William A. Denny,∥ and Kurt Wüthrich*,‡

Institut für Molekularbiologie und Biophysik, Eidgenössische Technische Hochschule—Hönggerberg, CH-8093 Zürich, Switzerland, and Cancer Research Laboratory, School of Medicine, University of Auckland, Private Bag, Auckland, New Zealand

Received June 15, 1988; Revised Manuscript Received September 21, 1988

ABSTRACT: The conformation at the dA-dT junction in d-(AAAAATTTTT)$_2$ was investigated by using a variety of phase-sensitive two-dimensional nuclear magnetic resonance experiments at 500 MHz for detailed studies of the deoxyribose ring puckers. Conformational constraints were collected from two-dimensional nuclear Overhauser enhancement spectra recorded with short mixing times and from quantitative simulations of the cross-peaks in two-dimensional correlated spectra. Overall, the decamer duplex adopts a conformation of the B-DNA type, and for dA_4 and dA_5 the pseudorotation phase angle P is in the standard range 150–180°. The deoxyribose puckers for the other nucleotides deviate significantly from the standard B-DNA structure. Spectrum simulations assuming either static deviations from standard B-DNA or a simple two-state dynamic equilibrium between the C2′-endo and C3′-endo forms of the deoxyribose were used to analyze the experimental data. It was thus found that the ring pucker for dT_6 deviates from the regular C2′-endo form of B-DNA by a static distortion, with the pseudorotation phase angle P in the range 100–130°, and a similar value of P is indicated for dT_7. For the peripheral base pairs dynamic distortions of the C2′-endo form of the deoxyribose were found. In agreement with recent papers on related duplexes containing $(dA)_n$ tracts, we observed prominent nuclear Overhauser effects between adenine-2H and deoxyribose-1′H, which could be largely due to pronounced propeller twisting as observed in the crystal structures of $(dA)_n$-containing compounds.

Three-dimensional structures of synthetic oligodeoxynucleotide duplexes containing $(dA)_n$ tracts attract increasing interest, which recently motivated a series of investigations by NMR[1] (Behling et al., 1987; Roy et al., 1987; Kintanar et al., 1987; Sarma et al., 1988), single-crystal X-ray diffraction (Nelson et al., 1987; Coll et al., 1987), and optical spectroscopic techniques [e.g., Taillendier et al. (1987), Edmondson (1987), and Benevides et al. (1988)]. This interest is related to various observations that appear to relate $(dA)_n$ tracts with important functional properties of DNA. Thus, studies of the electrophoretic mobilities in polyacrylamide gels of DNA fragments isolated from the kinetoplast body of tropical parasites (Simpson, 1979; Challberg & Englund, 1980; Englund et al., 1982; Marini et al., 1982; Levene & Crothers, 1983; Wu & Crothers, 1984; Hagerman, 1984, 1986; Koo et al., 1986) or from the origin of replication of bacteriophage λ (Zahn & Blattner, 1985) and of synthetic DNA fragments containing adenine tracts of different length phased differently along the DNA (Koo et al., 1986) indicated that $(dA)_n$ stretches introduce bending of double-helical DNA (Wu & Crothers, 1984; Hagerman, 1986; Koo et al., 1986; Koo & Crothers, 1987). On the basis of unusual spectroscopic properties of poly(dA)·poly(dT), it was also suggested that certain structural features of this compound might be related with the fact that it cannot be used to reconstitute nucleosomes (Rhodes & Klug, 1981; Travers & Klug, 1987). Studies of $(dA)_n$-containing oligonucleotides may also be of interest with regard to the structure of poly(dA)·poly(dT), which has been the subject of some controversy (Arnott et al., 1983; Thomas & Peticolas, 1983; Jollès et al., 1985; Behling & Kearns, 1986; Katahira et al., 1986; Alexeev et al., 1987a,b; von Kitzing & Diekmann, 1987; Taillendier et al., 1987; Patapoff et al., 1988).

Different explanations were offered for the implicated bending of DNA duplexes at or near the $(dA)_n$ tracts (Trifonov, 1986). For example, it was suggested that $(dA)_n$ segments retain the B-DNA conformation but undergo unusual interactions with the nearest or next-nearest base pairs or that there is potential structural polymorphism at the $(dA)_n$ tracts and the junctions with the adjacent DNA segments (Koo et al., 1986). Earlier studies with oligonucleotides indicated that

† This work was supported by the Swiss National Science Foundation (Project 3.198.85), the Swiss Cancer League (to W.L.), and the Auckland Division of the Cancer Society of New Zealand. Presented in part at the I Reunion Española de Biofisica, Sitges, Spain, Oct 1–4, 1986.

‡ Eidgenössische Technische Hochschule—Hönggerberg.

§ Present address: Departamento de Quimica Fisica, Facultad de C.Quimicas, Universidad de Valencia, Burjassot (Valencia), Spain.

∥ University of Auckland.

Present address: Department of Pharmaceutical Research, Hoffmann-La Roche & Co., Ltd., CH-4002 Basel, Switzerland.

⊥ Present address: Department of Molecular Biology, Scripps Clinic and Research Foundation, La Jolla, CA 92037.

[1] Abbreviations: NMR, nuclear magnetic resonance; FID, free induction decay; 1D, one-dimensional; 2D, two-dimensional; COSY, two-dimensional correlated spectroscopy; 2Q, two-quantum; 2QF-COSY, two-quantum-filtered COSY; RELAYED-COSY, two-dimensional relayed coherence transfer spectroscopy; TOCSY, two-dimensional total correlation spectroscopy; NOE, nuclear Overhauser effect; NOESY, two-dimensional NOE spectroscopy; ppm, parts per million; IR, infrared; $d_i(X;Y)$, intranucleotide distance between the protons X and Y; $d_s(X;Y)$, distance between the protons X and Y located in sequentially neighboring nucleotides, where the direction from X to Y is always 5′ to 3′; $d_{ps}(X;Y)$, distance between the protons X and Y located in adjoining, stacked base pairs.

0006-2960/89/0428-1462$01.50/0

maximal bending occurred for correctly phased $(dA)_n$ tracts with $n = 5$ or 6 and that the bending is at a maximum if $(dA)_n$ is flanked by dT at its 3′ end or by dC at its 5′ end (Koo et al., 1986). In the crystal structures of d-(CGCAAAAAAGCG)·d-(CGCTTTTTTGCG) and d-(CGCAAATTTGCG)$_2$, the runs of AT base pairs have outstandingly large propeller twists averaging ca. 20° and vanishingly small base roll angles (Coll et al., 1987; Nelson et al., 1987), and it was suggested that this intrinsic structural property of $(dA)_n$ tracts might be responsible for DNA bending, with maximum bending for $n = 5$. The presence of pronounced propeller twist appears to be manifested by the observation of NOEs between adenine-2H and deoxyribose-1′H in solutions of oligonucleotides containing $(dA)_n$ segments (Kintanar et al., 1987; Roy et al., 1987).

This paper describes a study of the solution structure of the decadeoxynucleotide d-(AAAAATTTTT)$_2$, which was initiated several years ago (Celda et al., 1986). The aforementioned NOEs between adenine-2H and deoxyribose-1′H were observed also in this compound, indicating the same structure type as for the other recently studied related oligonucleotide duplexes. Our interest was primarily focused on the structure of the backbone at the dA-dT junction. Roy et al. (1987) had previously concluded on the basis of partial resonance assignments for the nonlabile protons and NOESY spectra recorded at 400 MHz with mixing times of 100 and 300 ms that in the closely related duplex d-(AAAAAATTTTTT)$_2$ the conformation at the junction is "significantly different from the rest of the molecule". The goal of the present study with d-(AAAAATTTTT)$_2$ was to obtain more precise information. Nearly complete sequence-specific assignments were obtained, and the structural constraints obtained from NOESY spectra recorded with very short mixing times were complemented by data on the spin–spin coupling constants obtained from quantitative simulations of COSY spectra.

Materials and Methods

The decadeoxynucleoside nonaphosphate d-(AAAAATTTTT)$_2$ was synthesized by a modification of the phosphotriester method in liquid phase, starting from the commercially available deoxynucleosides (Fluka AG). The amino group of dA was benzoylated by the transient protection method of Jones and co-workers (Ti et al., 1982). All other procedures used have been described in detail elsewhere (Chazin et al., 1986; Denny et al., 1982). The decanucleotide was employed as the sodium salt. For the NMR experiments the decanucleotide was dissolved in 400 μL of H_2O or ^2H_2O containing 0.1 M NaCl, 0.05 M phosphate buffer, and 0.1% (w/v) NaN_3, pH 7.0. The concentration of the DNA was 1.2 mM in duplex. The ^1H NMR spectra were obtained at 500 MHz on a Bruker WM-500 spectrometer equipped with an ASPECT 3000 computer. A description of the individual NMR epxeriments used has been deposited as supplementary material.

Quantitative measurements of the ^1H–^1H scalar couplings in the deoxyribose rings were obtained by simulation of the cross-peaks in a 2QF-COSY spectrum (Rance et al., 1983) recorded with acquisition times of 41 ms in t_1 and 270 ms in t_2. The data were multiplied with sine-bell functions in both dimensions and then zero-filled to obtain a digital resolution of 0.98 Hz/point in ω_2 and 4.88 Hz/point in ω_1. The SPHINX and LINSHA programs (Widmer & Wüthrich, 1986) were used for the simulations. These programs calculate 2D correlated spectra of strongly coupled spin systems and account for the parameters influencing the 2D line shapes, i.e., the natural line width, the truncation of the FID, and the digital filter functions. The spin systems considered in the simulations comprised 1′H, 2′H, 2″H, 3′H, 4′H, and the phosphorus spin ^{31}P connected to the 3′-position.

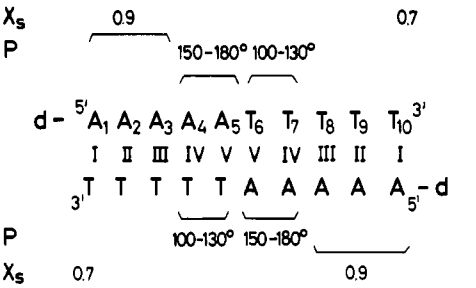

FIGURE 1: Structure of d-(AAAAATTTTT)$_2$. The Roman numerals reflect the twofold symmetry observed for the solution conformation of the duplex. The deoxyribose conformations in d-(AAAAATTTTT)$_2$ resulting from the present study are indicated above and below each strand. P is the pseudorotation phase angle in a static deoxyribose conformation, and X_S indicates the population of the C2′-endo ring pucker in a dynamic equilibrium with the C3′-endo form.

Table I: Relative NOESY Cross-Peak Intensities in d-(AAAAATTTTT)$_2$[a]

nucleotide[b]	$d_i(1';4')$	$d_i(6,8;2')$[c]	$d_s(2'';6,8)$[c]	$d_s(2;1')$	$d_{ps}(A_n,2;T_{12-n}1')$
dA_1	50	*d*			
dA_2	40	*d*	*d*	*f*	
dA_3	40	80	20	*f*	
dA_4	40	80	20	*f*	
dA_5	40	40	80	5	
dT_6	320	40	40	10	
dT_7	160	40	40		10
dT_8	(320)[e]	40	40		10
dT_9	(320)[e]	40	40		20
dT_{10}	40	40	20		5

[a] Values derived from a NOESY spectrum recorded with τ_m = 40 ms, using a DNA sample of 1.2 mM in duplex, 100 mM NaCl, 50 mM phosphate buffer, pH 7.0, T = 293 K. [b] For the sequential NOEs this column lists the nucleotide with the higher sequence number. [c] The NOEs corresponding to $d_i(6,8;2'')$ and $d_s(2';6,8)$ were too weak to be observed. [d] Not measured because of spectral overlap. [e] Parentheses indicate uncertainty due to spectral overlap. [f] Too weak to be observed.

Results

In the 1D ^1H NMR spectra of the decanucleotide d-(AAAAATTTTT)$_2$ the presence of only five methyl resonances and four imino proton lines showed that the twofold symmetry of the chemical structure is preserved in the solution conformation (Figure 1). The imino proton line corresponding to the peripheral base pairs I was not observed, presumably because of fraying of the duplex at the chain ends. Chemical shift versus temperature profiles (not shown) showed that a duplex structure was present over the temperature range 281–303 K, and therefore 293 K was selected for all further experiments.

(*a*) *Sequence-Specific Resonance Assignments.* For the resonance assignments, recently described procedures (Chazin et al., 1986) were employed, which follow a similar strategy as in earlier work [e.g., Feigon et al. (1982, 1983), Hare et al. (1983), Scheek et al. (1983, 1984), and Weiss et al. (1984a)]. A description of the assignments, the NMR spectra used, and the chemical shift table have been deposited as supplementary material.

(*b*) *Structural Constraints from NOE Measurements.* A semiquantitative evaluation of the cross-peak intensities corresponding to $d_i(6,8;2')$ and $d_s(2'';6,8)$ is presented in Table I. The fact that these NOEs are more intense than those corresponding to $d_i(6,8;2'')$ and $d_s(2';6,8)$ is a clear-cut, qualitative indication that d-(AAAAATTTTT)$_2$ has a B-DNA

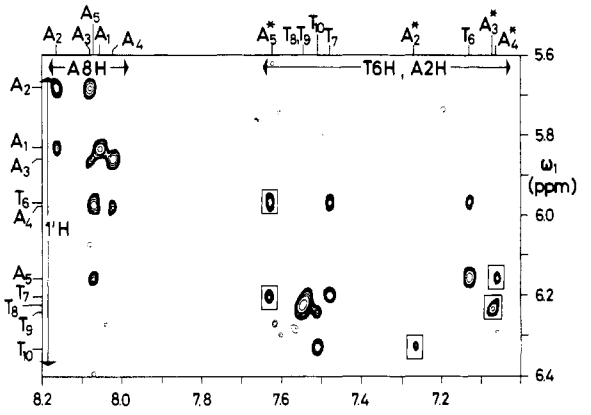

FIGURE 2: Absorption mode NOESY spectrum at 500 MHz of d-(AAAAATTTTT)$_2$ recorded in ^2H_2O with a 100-ms mixing time. The spectral region (ω_1 = 5.6–6.4 ppm, ω_2 = 7.0–8.2 ppm) containing cross-peaks between 1′H and base protons is shown. The chemical shift ranges for these protons are indicated on the left and at the top. Sequence-specific assignments are indicated on the left for 1′H and at the top for the base protons 6H, 8H, and 2H of adenine, where the latter are identified by a star. The five framed cross-peaks between adenine-2H and 1′H are discussed in the text and in Table I.

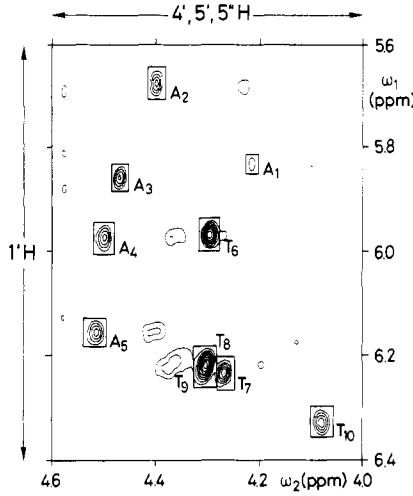

FIGURE 3: Absorption mode NOESY spectrum at 500 MHz of d-(AAAAATTTTT)$_2$ recorded in ^2H_2O with a 40-ms mixing time. The spectral region (ω_1 = 5.6–6.3 ppm, ω_2 = 4.0–4.6 ppm) containing cross-peaks between 1′H and 4′H, 5′H, and 5″H is shown. The chemical shift ranges for these protons are indicated on the left and at the top. Sequence-specific assignments are indicated for the boxed 1′H–4′H intranucleotide cross-peaks.

conformation type (Wüthrich, 1986). Inspection of Table I reveals that for dA$_1$–dA$_4$ the relative intensities of the NOEs corresponding to d_i(6,8;2′) and d_s(2″;6,8) and their ratios are different from the corresponding data for the dTs and that unique values were observed for dA$_5$. Among the additional NOESY cross-peak intensities (Table I) those between A2H and 1′H are of special interest since sequential intrastrand as well as interstrand NOEs between these protons were observed (Figure 2, Table I). Furthermore, since the distance between the deoxyribose protons 1′H and 4′H depends strongly on the sugar pucker (Wüthrich, 1986), NOEs between these protons (Figure 3, Table I) are also of interest for the ensuing discussions on the molecular conformation.

(*c*) *Determination of the Deoxyribose ^1H–^1H Spin–Spin Coupling Constants by Quantitative Simulations of 2QF-COSY Cross-Peaks.* A visual inspection of the 2QF-COSY cross-peaks in d-(AAAAATTTTT)$_2$ clearly shows differences between the individual nucleotides. This is illustrated by Figures 4 and 5, which show the cross-peaks 1′H–2′H and

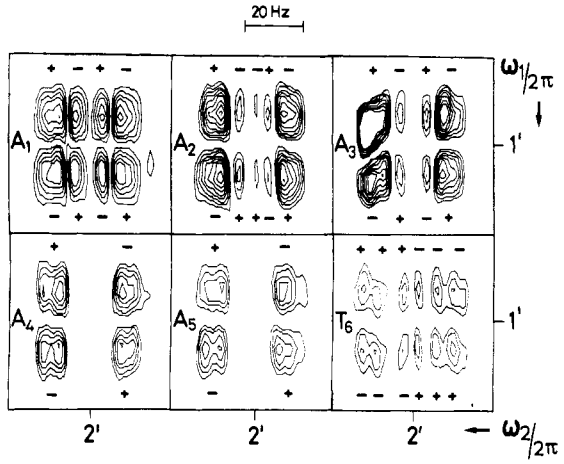

FIGURE 4: Experimental 1′H(ω_1)–2′H(ω_2) cross-peaks of dA$_1$–dA$_5$ and dT$_6$ in the 2QF-COSY spectrum of d-(AAAAATTTTT)$_2$. The data handling used (described in supplementary material) resulted in a digital resolution of 0.98 Hz/point in ω_2 and 4.88 Hz/point in ω_1, respectively. The contours are plotted at linearly increasing levels. Positive and negative peak components are distinguished by the signs + and −. 1′ and 2′ identify the chemical shift positions of the corresponding protons, and the frequency scale is also indicated. Note that in the A$_3$ multiplet the components on the left are overlapped with the 1′H–2″H cross-peak of dA$_1$.

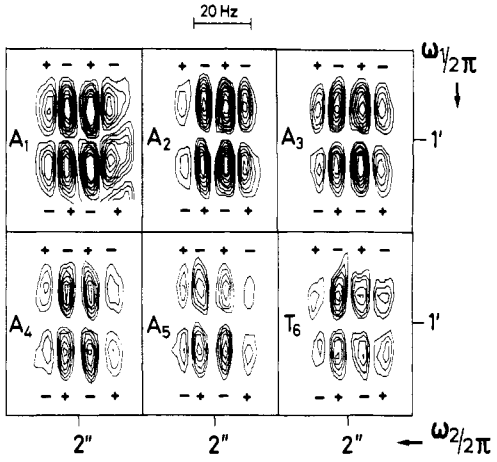

FIGURE 5: Experimental 1′H(ω_1)–2″H(ω_2) cross peaks of dA$_1$–dA$_5$ and dT$_6$ in the 2QF-COSY spectrum of d-(AAAAATTTTT)$_2$; same spectrum and same presentation as in Figure 4. Note that the components on the right in the dA$_1$ cross-peak overlap with the 1′H–2′H cross-peak of dA$_3$.

1′H–2″H of the five adenines and of dT$_6$, which are well separated in the spectrum. Because of the limited digital resolution along ω_1, where only two fine structure components are resolved, the analysis was primarily concentrated on the resolved features along ω_2. (In Figures 4 and 5 these are the coupling interactions with 2′H and 2″H, respectively. The corresponding cross-peaks on the other side of the diagonal, with 1′H along ω_2, were also analyzed.) In Figure 4 all the 1′H–2′H cross-peaks contain two intense outer components along ω_2, with an indication of an unresolved in-phase splitting due to passive couplings. Four types of different peak patterns are seen for the central components. For dA$_1$ there are four major components, which alternate in phase and have nearly equal intensity. For dA$_2$ and dA$_3$ the phases and frequency positions of the individual fine structure components along ω_2 are approximately the same as for dA$_1$, but the intensities of the central components are considerably decreased. An additional weak component in the center of the dA$_2$ multiplet is due to strong coupling between 2′H and 2″H. For dA$_4$ and dA$_5$ the inner components are below the noise level. Since the

in-phase splitting of the outer components is resolved approximately to the same extent as for dA_1 to dA_3, this appears not to be solely a consequence of broader line widths. dT_6 is similar to dA_2, except that the inner components have different phases, and the peripheral components are weaker and show better resolution of the passive couplings. Less variation is seen among the 1′H–2″H cross-peaks of the same six nucleotides (Figure 5). All of them show very similar fine structures, with four resolved components along the 2″H dimension. Similarly, the four well separated 2′H–3′H cross-peaks of dA_1, dA_2, dA_5, and dT_6 (Widmer, 1987; not shown here) all had closely similar appearance.

None of the experimental 1′H–2′H, 1′H–2″H, or 3′H–2′H cross-peaks exhibited the complete eight-component multiplet for 2′H or 2″H, which is expected for spins with three nondegenerate couplings. The frequency positions of the four to six fine structure components that were resolved showed the influence of cancellation and amalgamation effects characteristic of mutually overlapping positive and negative components in antiphase multiplets, so that the peak-to-peak separations do not always coincide with the corresponding coupling constants (Neuhaus et al., 1985; Wüthrich, 1986). These experimental artifacts were taken into account by the use of the proper parameters in spectrum simulations using the programs SPHINX and LINSHA (see Materials and Methods for details). The deoxyribose spin systems considered in the simulations comprised 1′H, 2′H, 2″H, 3′H, 4′H, and the ^{31}P spin bound to the 3′-position. For the simulations of some of the 1′H–2′H and 1′H–2″H cross-peaks, a subsystem was used where 4′H and the ^{31}P spin were not considered. Weak coupling was assumed throughout, except between 2′H and 2″H, where the experimental chemical shift difference was used in the calculations. In order to find parameter sets corresponding to the observed cross-peak fine structures and to evaluate the precision with which the individual spin–spin coupling constants could be determined by using the experiments of Figures 4 and 5, sets of simulations were calculated with systematic variation of the coupling constants for the spin observed along ω_2. Since they do not directly affect the fine structure along ω_2, those parameters that are effective only along the less well resolved ω_1 axis were kept constant for all calculations of a given cross-peak. A check on the internal consistency of the spectrum simulations was obtained from the fact that the same spin–spin coupling constants are manifested along ω_2 in different cross-peaks, e.g., in 1′H(ω_1)–2′H(ω_2) and 3′H(ω_1)–2′H(ω_2).

In the simulations of the 1′H(ω_1)–2′H(ω_2) cross-peaks, the coupling constants $^3J_{1'2'}$, $^2J_{2'2''}$, and $^3J_{2'3'}$ were varied while all other coupling constants of the spin systems were kept fixed (see caption to Figure 6). The range of values for the variable parameters was restricted by the following considerations. Since $^2J_{2'2''}$ in deoxyribose rings is always close to −14.0 Hz [e.g., Davies and Danyluk (1974) and Davies (1978)], simulations were done for −13.0, −14.0, and −15.0 Hz. For $^3J_{1'2'}$ the upper bound of the range considered corresponds to the maximum for vicinal ^{1}H–^{1}H coupling constants that is commonly observed. The lower bound of 9.2 Hz for the range of $^3J_{1'2'}$ values and the range from 4.3 to 8.5 Hz for $^3J_{2'3'}$ were based on the considerations that the splitting of the outermost fine structure components in Figures 4 and 5 is in-phase and must therefore correspond to $^3J_{2'3'}$ and that the overall width along ω_2 of the multiplets 1′H(ω_1)–2′H(ω_2) and 3′H(ω_1)–2′H(ω_2) is determined by the sum of $^3J_{1'2'} + {}^2J_{2'2''} + {}^3J_{2'3'}$. Within these ranges the coupling constants $^3J_{1'2'}$ and $^3J_{2'3'}$ were changed independently in 0.7-Hz increments. For all spin

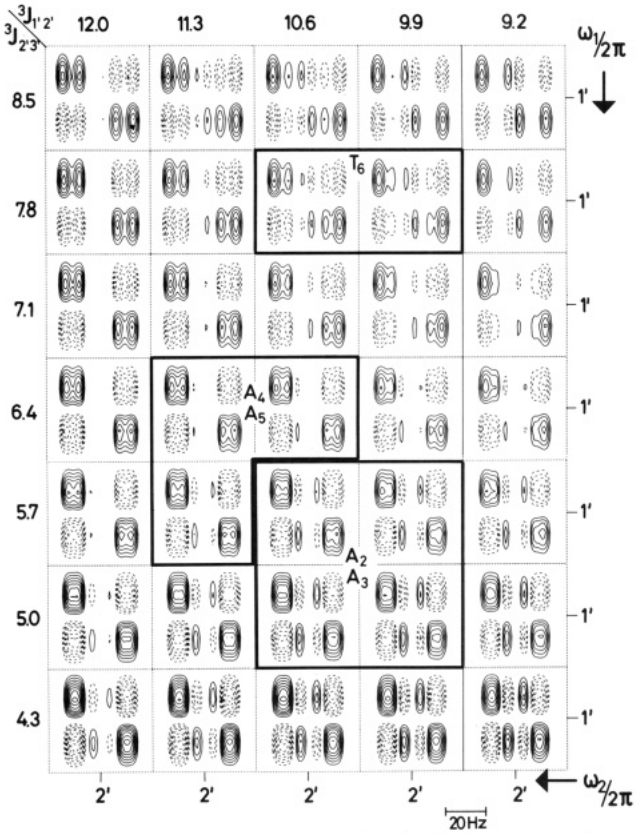

FIGURE 6: Simulated 1′H(ω_1)–2′H(ω_2) 2QF-COSY cross-peaks of deoxyribose. The coupling constants $^3J_{1'2'}$ and $^3J_{2'3'}$ were systematically varied as indicated at the top and on the left. The other coupling constants are $^2J_{2'2''}$ = −13.0 Hz, $^3J_{1'2''}$ = 5.6 Hz, $^3J_{2''3'}$ = 1.0 Hz, $^3J_{3'4'}$ = 2.0 Hz, and $^3J_{3'P}$ = 5.6 Hz. 2″H is 240 Hz to lower field than 2′H, and for all other combinations of protons weak coupling was assumed. In both dimensions the full line width at half-height was 9.0 Hz, and an exponential decay of the free induction was used. The acquistion times, the filter functions, and the digital resolution in both dimensions are the same as in the experimental spectrum of d-(AAAAATTTTT)$_2$ (see caption to Figure 4 and supplementary material). In this and in all other figures showing simulated cross-peaks, contours are plotted at linearly increasing positive (solid lines) and negative (broken lines) levels. 1′ and 2′ identify the chemical shifts of the corresponding protons. The thick frames enclose the best fits with the experimentally observed cross-peak fine structures for dA_2 and dA_3, dA_4 and dA_5, and dT_6, respectively, as indicated in the figure.

systems except dT_{10} (see below) the chemical shift difference $\Delta\nu_{2'2''}$ was sufficiently large to be read from the experimental spectrum. In Figure 6 the strong coupling between these two protons is manifested by slight deviations of the cross-peaks from D_2 symmetry, and the extra peak in the center of the 1′H–2′H cross-peak of dA_2 (Figure 4) was also reproduced with $\Delta\nu_{2'2''}$ = 55 Hz (not shown). In the representation of the cross-peaks with the program LINSHA the same acquisition times, window functions, and digital resolution as in the experiment were used. For the full line width at half-height the range from 5 to 10 Hz was tried in steps of 1 Hz. The line width affects mainly the overall intensity of the cross-peaks, whereas the peak patterns are not very sensitive to this parameter.

In Figure 6 those simulations are framed that represent the best fits with the different experimental cross-peaks. Similar studies to that of Figures 4 and 6 were done for the 1′H(ω_1)–2″H(ω_2) and 3′H(ω_1)–2′H(ω_2) cross-peaks (Widmer, 1987; not shown here). The 3′H–2′H cross-peaks are much less sensitive to changes in the coupling constants than the 1′H–2′H cross-peaks (see also Figure 9), so that they do not allow establishment of tighter bounds on the values for the

Table II: ^1H–^1H Coupling Constants in d-(AAAAATTTTT)$_2$[a]

nucleotide	$^3J_{1'2'}$	$^3J_{1'2''}$	$^2J_{2'2''}$	$^3J_{2'3'}$	$^3J_{2''3'}$
dA_1	8.5–9.9	5.0–6.4	−14.0 to −14.5	5.0	<3.0
dA_2	9.2–10.6	5.0–5.7	−13.0 to −14.5	5.0–5.7	<3.0
dA_3	9.2–10.6	5.0–5.7	−13.0 to −14.5	5.0–5.7	<3.0
dA_4	9.2–11.3	5.0–6.4	−13.0 to −14.5	5.7–6.4	<3.0
dA_5	9.2–11.3	5.0–6.4	−13.0 to −14.5	5.7–6.4	<3.0
dT_6	9.2–10.6	5.0–6.4	−13.0 to −14.5	7.8	<3.0
dT_7–dT_9	(9.9–10.6)[b]	(5.0–6.4)[b]	(−13.0 to −14.5)[b]	(7.8)[b]	(<3.0)[b]
dT_{10}	(7.0)[b]	(6.3)[b]	(−13.5)[b]	(7.0)[b]	(3.4)[b]

[a] Derived from simulations of COSY cross-peaks of a d-(AAAAATTTTT)$_2$ sample with 1.2 mM in duplex, 100 mM NaCl, 50 mM phosphate buffer, pH 7.0, T = 293 K. [b] Numbers in parentheses indicate that the range of values is uncertain (see text).

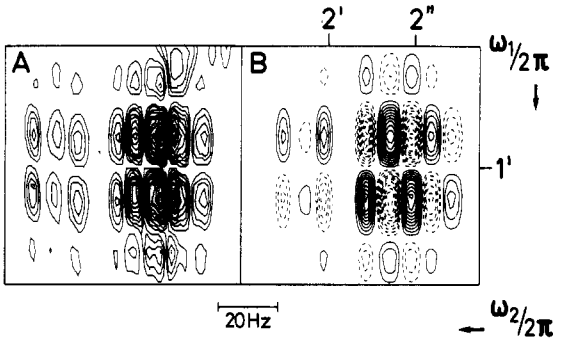

FIGURE 7: Experimental and simulated 2QF-COSY cross-peaks of dT_{10} in d-(AAAAATTTTT)$_2$. The presentation and the acquisition and processing parameters are the same as in Figures 4–6. The coupling constants used for the simulation are $^3J_{1'2'}$ = 7.0 Hz, $^3J_{1'2''}$ = 6.3 Hz, $^2J_{2'2''}$ = −13.5 Hz, $^3J_{2'3'}$ = 7.0 H, $^3J_{2''3'}$ = 3.4 Hz, $^3J_{3'4'}$ = 2.0 Hz, and $^3J_{3'P}$ = 5.6 Hz. 2"H is 29.0 Hz to higher field than 2'H. The line width was 5.5 Hz.

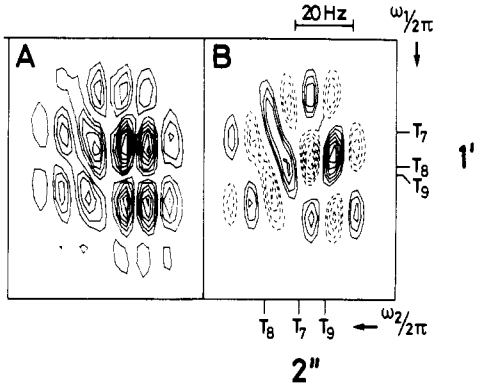

FIGURE 8: 1'H(ω_1)–2"H(ω_2) 2QF-COSY cross-peaks of dT_7–dT_9 in d-(AAAAATTTTT)$_2$. (A) Experiment. (B) Superposition of three identical cross-peaks computed with the parameters $^3J_{1'2''}$ = 6.7 Hz, $^2J_{2'2''}$ = −14.5 Hz, $^3J_{1'2'}$ = 10.6 Hz, $^3J_{2'3'}$ = 5.7 Hz, $^3J_{2''3'}$ = 0.7 Hz, and 2"H 240 Hz to lower field than 2'H. Relative to dT_9, the 1'H and 2"H chemical shifts for dT_7 are −15 and +9 Hz, respectively, and for dT_8 −3 and +21 Hz, respectively, where negative numbers indicate upfield shifts.

individual coupling constants than those corresponding to the frames in Figure 6. Similarly, the 1'H–2"H cross-peaks are less sensitive to a change of the J coupling parameters than the 1'H–2'H cross-peaks, which coincides with the smaller variations among the different nucleotides observed in Figure 5 when compared to Figure 4. Simulations for the cross-peaks on the other side of the diagonal, e.g., 2'H(ω_1)–1'H(ω_2) and 2'H(ω_1)–3'H(ω_2), confirmed the conclusions from Figure 6, except for the values of $^3J_{1'2'}$, which were found to be ca. 0.7 Hz smaller in the best fits of these experimental cross-peaks. This was taken into account by extending the range for the coupling constants given in Table II.

For dT_{10} the strong coupling of the C2'-protons prevented an independent treatment of the 1'H–2'H and 1'H–2"H cross-peaks. All the coupling constants $^3J_{1'2'}$, $^3J_{1'2''}$, $^2J_{2'2''}$, $^3J_{2'3'}$, and $^3J_{2''3'}$ therefore had to be varied in the same simulations (Figure 7), and the chemical shift difference could not be read directly from the experimental spectra and therefore had to be fitted as well. In this situation only estimates for the values of the individual coupling constants could be obtained, with the only significant differences from the nonterminal nucleotides being the smaller value for $^3J_{1'2'}$ (Table II) and the smaller line width. Figure 7 shows that with the parameters listed in the caption a satisfactory fit of this complex cross-peak was achieved.

The cross-peaks of dT_7, dT_8, and dT_9 are strongly overlapped (e.g., Figure 8A), which precluded a meaningful simulation of the individual cross-peaks. We therefore examined only how the experimental spectral features resulting from these three nucleotides could best be fitted by superpositions of three identical cross-peaks of any of the types observed for the other deoxyriboses. An optimal fit was obtained by variation of the relative chemical shifts, as indicated in the caption to Figure 8. Overall, comparison with these simulated peak superpositions indicates that the experimental spectra would be compatible with similar cross-peak fine structures as those for dA_1–dA_5 and dT_6, with evidence for closest coincidence with dT_6.

The deoxyribose spin–spin coupling constants determined by visual fitting of the spectrum simulations (Figures 6–8) with the experiments (Figures 4, 5, and 8) are listed in Table II. The ranges given in the table correspond basically to the framed regions in Figure 6, which were extended beyond the limits identified by the frames in those instances where the simulation of different cross-peaks resulted in somewhat different values for a particular parameter.

Discussion

In DNA duplexes containing natural nucleotides (i.e., for example, not carrying nitroxide spin labels), there are presently no NMR parameters that could be directly related to bending of the double helix. Therefore, the following analysis is focused on the identification of unusual local conformational features in individual nucleotides, which might serve on an empirical line as indicators of unusual traits of the global molecular structure. We started with the assumption that the d-AAAAATTTTT duplex is of the B-DNA type, which is supported by the observation that at short mixing times only the NOESY cross-peaks corresponding to the ^1H–^1H distances d_i(6,8;2') and d_s(2";6,8) were seen, whereas the d_i(6,8;2") and d_s(2';6,8) connectivities were absent (Table I) (Wüthrich, 1986). On this basis we then investigated if there were structurally significant deviations of individual ^1H–^1H scalar coupling constants or NOESY cross-peak intensities from the standard values expected for B-DNA.

(a) Deoxyribose Ring Puckers in d-(AAAAATTTTT)$_2$ Viewed by Measurements of ^1H–^1H Scalar Coupling Con-

stants. Realizing that the NMR parameters collected in the present study can be directly related only to strictly local features of the conformation of d-(AAAAATTTTT)$_2$ and considering that the distance constraints obtained from NOESY experiments are presently still primarily useful for characterizing the global features of a macromolecular conformation rather than the local details of the three-dimensional structure that would be of interest here (Wüthrich, 1986), we concentrated our efforts on a structural interpretation of ^{1}H–^{1}H scalar couplings in the deoxyribose rings. This idea is a priori not original, since spin–spin coupling constants have been analyzed in a large number of mononucleotides and small oligonucleotides [e.g., Altona (1982)], and more recent studies also described the use of spin–spin coupling constants for investigations of DNA duplexes (Hosur et al., 1986; Chary et al., 1987; Rinkel & Altona, 1987). However, relative to these latter projects the present measurements of ^{1}H–^{1}H coupling constants by complete simulation of the cross-peaks should be more reliable, since the simulations account also for distortions of the multiplet fine structure by the filter functions used, large line widths, truncation effects, etc. (Neuhaus et al., 1985; Wüthrich, 1986). Hosur et al. (1986) proposed to use the absolute value COSY cross-peak intensities to assess the relative size of the active couplings in the different nucleotides of a DNA duplex, assuming that the passive couplings and the line width have the same influence for a given type of cross-peak in all nucleotides of the molecule. Rinkel and Altona (1987) derived sums of coupling constants from the partially resolved multiplets in absolute value COSY cross-peaks and from one-dimensional spectrum simulations using idealized narrow resonance lines. In the real cases where the resonance lines are rather broad, such as in d-(AAAAATTTTT)$_2$, the in-phase splittings are not resolved and the frequency differences between the peripheral multiplet components would then be difficult to measure with this technique.

To obtain a basis for the structural analysis of the spin–spin coupling data, we started from a recent compilation of hypothetical cross-peak patterns (Widmer & Wüthrich, 1987). Using the same conditions as in the simulations of the experimental cross-peaks (Figures 6–8), these earlier computations of ^{1}H–^{1}H COSY cross-peaks were repeated and expanded in scope. On the one hand, cross-peak multiplets were simulated for a rigid deoxyribose ring, with the conformation characterized by the pseudorotation phase angle, P, and the pucker amplitude, Φ_m, defining the endocyclic torsion angles, Φ_j (Altona & Sundaralingam, 1972, 1973):

$$\Phi_j = \Phi_m \cos (P + 4\pi(j-2)/5); \quad j = 0\text{–}4 \qquad (1)$$

The coupling constants corresponding to $\Phi_m = 40°$ and selected values of P were used to simulate the cross-peaks C1′H–C2′H, C1′H–C2″H, C3′H–C2′H, and C3′H–C2″H (Figure 9; Figure 10 with $X_S = 0.0$ and 1.0). On the other hand, simulations were calculated for the same cross-peaks by using a dynamic model for the deoxyribose ring, where only the two conformation states with $P_N = 9°$ and $\Phi_m = 40°$ and $P_S = 171°$ and $\Phi_m = 40°$, respectively, would be populated. P_N corresponds closely to the C3′-endo conformation of A-DNA, and P_S is near C2′-endo of B-DNA (Saenger, 1984). Rapid interconversion between these two limiting deoxyribose conformations is assumed, with the fractional populations X_S and X_N. The effective coupling constants, J_{ik}^{eff}, are

$$J_{ik}^{eff} = X_N J_{ik}^{N} + X_S J_{ik}^{S}; \quad X_N + X_S = 1 \qquad (2)$$

J_{ik}^{N} and J_{ik}^{S} represent the coupling constants between the spins

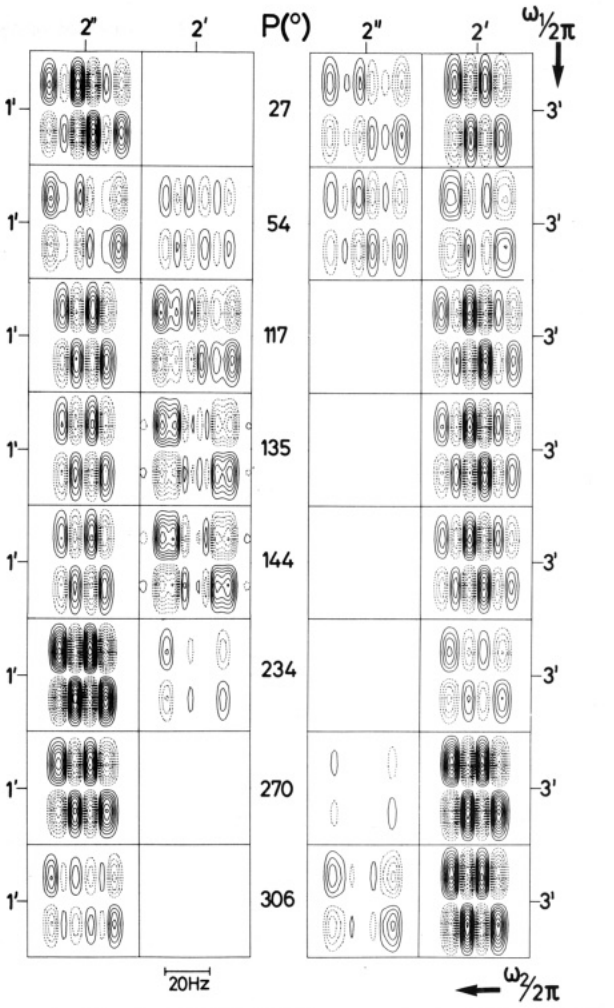

FIGURE 9: Simulated 2QF-COSY cross-peaks for different rigid conformers of deoxyribose characterized by a sugar pucker amplitude of 40° and the pseudorotation phase angles, P, indicated in the figure. The 1′H–2′H, 1′H–2″H, 2′H–3′H, and 2″H–3′H cross-peaks are shown. The chemical shifts of dA$_5$ in d-(AAAAATTTTT)$_2$ are used. The full line width at half-height is 9.0 Hz, and the other line-shape parameters are the same as in Figure 6 (see also Materials and Methods). The coupling constants $^2J_{2'2''}$ and $^3J_{3'P}$ are −13 and 5.8 Hz, respectively, and the other coupling constants (Hz) are shown below (Rinkel & Altona, 1987). The frequency scale is indicated in the figure. On the sides and at the top, 1′, 3′, 2′, and 2″ identify the chemical shifts of the corresponding protons. The contours are plotted at linearly increasing positive (solid lines) and negative (broken lines) levels. Empty boxes indicate that the corresponding cross-peak is too weak to show contours.

P (deg)	$^3J_{1'2'}$	$^3J_{1'2''}$	$^3J_{2'3'}$	$^3J_{2''3'}$	$^3J_{3'4'}$
27	2.4	8.6	7.1	9.8	8.8
54	5.4	9.0	8.7	7.8	8.7
117	10.3	5.5	8.1	1.5	4.6
135	10.6	5.0	6.6	1.2	2.8
144	10.6	4.9	6.0	1.2	2.1
234	5.0	7.0	6.0	1.2	1.0
270	1.9	6.8	7.6	3.6	1.2
306	1.2	6.3	7.4	7.8	3.7

i and k in the N or S conformations, respectively. Cross-peaks were computed by using different sets of J_{ik}^{eff} values obtained with eq 2 (Figure 10). Figures 9 and 10 show which of the ^{1}H–^{1}H coupling constants are most sensitive to changes in conformation and therefore most useful for conformational studies. In the context of the present study the conformations near a standard A- or B-DNA and the region in between are of most interest. In both the static (Figure 9) and the dynamic (Figure 10) model the cross-peaks 1′H(ω_1)–2′H(ω_2) and 3′H(ω_1)–2″(ω_2) should enable an unambiguous qualitative

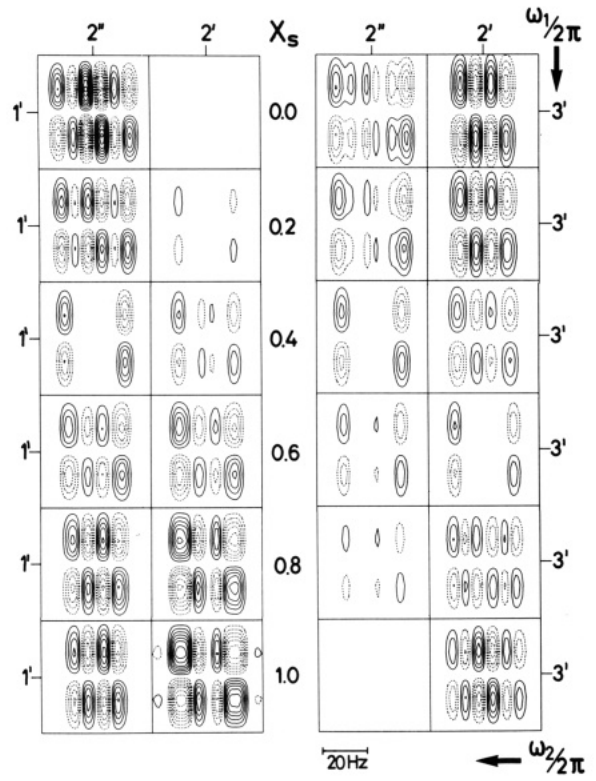

FIGURE 10: Simulated 2QF-COSY cross-peaks for dynamic states of a deoxyribose characterized by rapid interconversion between the two conformations with $P = 9°$ (N) and $P = 171°$ (S), for which the J values were taken from Rinkel and Altona (1987). The relative population of the S conformer, X_S, is given in the figure, and $X_N = 1 - X_S$. The line width, $^2J_{2'2''}$, and $^3J_{3'P}$ are the same as in Figure 9 and effective values of the other coupling constants (Hz) are shown below.

X_S	$^3J_{1'2'}$	$^3J_{1'2''}$	$^3J_{2'3'}$	$^3J_{2''3'}$	$^3J_{3'4'}$
0.0	1.5	7.7	6.5	10.3	8.5
0.2	3.3	7.2	6.2	8.6	7.0
0.4	5.0	6.7	5.8	6.8	5.5
0.6	6.8	6.1	5.5	5.1	4.0
0.8	8.5	5.6	5.1	3.3	2.5
1.0	10.3	5.1	4.8	1.6	1.0

distinction between A-DNA-type and B-DNA-type deoxyribose forms, with 1'H(ω_1)–2"H(ω_2) and 3'H(ω_1)–2'(ω_2) being much less sensitive to conformational changes and probably providing primarily supporting evidence for conclusions attained by using the other cross-peaks. Furthermore, comparison of the experimental data (Figures 4 and 5) with the simulated cross-peak fine structures in Figures 9 and 10 should enable a distinction between static or dynamic deviations of the structure of d-(AAAAATTTTT)$_2$ from a standard B-DNA form.

The experimental 1'H–2'H cross-peaks can be divided into four groups (Figures 4–6, Table II): (i) The J values for dA$_4$ and dA$_5$ indicate a static C2'-endo sugar conformation, with P in the range 150–180°. (ii) For dA$_1$, dA$_2$, and dA$_3$ both $^3J_{1'2'}$ and $^3J_{2'3'}$ are ca. 1 Hz smaller than for dA$_4$ and dA$_5$. The observed combinations of spin–spin coupling constants could be explained by either a static or a dynamic conformation change relative to dA$_4$ and dA$_5$. Following the static model the small decrease of $^3J_{2'3'}$ and $^3J_{1'2'}$ would indicate that the pseudorotation phase angle P is approximately 20° larger in dA$_1$–dA$_3$, since $^3J_{1'2'}$ decreases only for $P > 171°$ (captions to Figures 9 and 10). In particular for dA$_1$ the J values would indicate that P is in the range 171–198°, where the upper limit is given by the fact that we did not observe an increased value for $^3J_{1'2''}$. In the dynamic model (Figure 10) the combinations of J values observed for dA$_1$–dA$_3$ could be accommodated by small deviations from $X_S = 1$. For example, for dA$_1$ a value of $X_S = 0.9$ would give a satisfactory fit. While the presently available data do not allow a distinction to be made between the static and the dynamic models, the observation that the trend to smaller values of both $^3J_{1'2'}$ and $^3J_{2'3'}$ is most pronounced for dA$_1$ might be taken as an indication of a predominantly dynamic mechanism underlying the observed spectral changes. (iii) For dT$_6$ $^3J_{2'3'}$ is significantly larger than for dA$_1$–dA$_5$, whereas $^3J_{1'2'}$ is the same as for dA$_1$–dA$_5$. This set of coupling constants cannot be accommodated in the simple dynamic model of Figure 10, with the pure N and S conformations as the two limiting structures. It fits, however, a static structure with a pseudorotation phase angle P of 100–130° (see Figures 4, 9, and 10). A similar structure is implicated for dT$_7$–dT$_9$, but since the coupling constants were not determined individually and overall the experimental data for these sugar rings were limited by spectral overlap (Figure 8), this result is less well substantiated than that for dT$_6$. (iv) The combination of spin–spin coupling constants obtained from the analysis of the strongly coupled spectrum of dT$_{10}$ (Figure 7) can on be accommodated by a model assuming rapid exchange between different structures. A good fit was obtained with $X_S \approx 0.7$. Increased conformational flexibility of the 3'-terminal deoxyribose rings was reported also for other DNA duplexes (Orbons & Altona, 1986).

The precision of the determination of the J values, which are the basis for the aforementioned conclusions on the deoxyribose conformations in d-(AAAAATTTTT)$_2$, is a priori largely determined by the increments of the J values between the simulated fine structures used for the visual fits of the experiments. These in turn were selected so as to do justice to the dependence of the parameters in question on the changes of conformation. Also, the simulations covered large ranges of the individual parameters, so that we can be confident to have found unique sets of parameters to fit the experiments. However, there were also apparent artifacts in the experimental cross-peaks that we could not account for. For example, the in-phase splittings between the outer components of individual 1'H–2'H cross-peaks (Figure 4) were not identical, the separation of the anti phase components in the high-field and low-field portions of 1'H–2"H cross-peaks (Figure 5) differed by up to 1.5 Hz, or some components of the 3'H–2'H cross-peaks (Widmer, 1987) were tilted relative to the frequency axes. These features could not be eliminated by varying the phasing, and they could not be explained by strong coupling effects in the systems studied. Possible origins for these as yet unexplained spectral features, which were not explicitly considered in the simulations, could be deviations of the phases and the flip angles from the nominal values or different relaxation times for individual coherences. It should also be pointed out that large line widths had to be used to obtain satisfactory fits of the experiments (Figures 6–10), which also set limitations to the extent with which certain spectral details could be considered.

(*b*) *Structural Implications from the ^1H–^1H Overhauser Effects.* As was mentioned earlier, the NOEs used for obtaining the sequence-specific ^{1}H NMR assignments in d-(AAAAATTTTT)$_2$ (Table I) showed that the duplex has a right-handed, B-DNA-type structure. Of special interest for the present study then is that the NOESY cross-peak corresponding to the intranucleotide distance $d_i(1';4')$ is nearly an order of magnitude more intense for dT$_6$ than for dA$_1$–dA$_5$. A qualitatively similar result was obtained for dT$_7$ and is implicated for the less well resolved cross-peaks of dT$_8$ and

dT_9 (Figure 3, Table I). In a C2′-endo conformation with $P \approx 170°$, as it is indicated for dA and dA_5 by the J coupling constants, the distance $d_i(1';4')$ is ca. 3.1 Å. For the nonterminal dTs the relative NOESY cross-peak intensities then indicate that $d_i(1';4')$ is ca. 2.2–2.4 Å, which places the value of P between 60° and 120° [Figure 11.4 in Wüthrich (1986)].

The experimental finding that the NOE cross-peaks of dA_5 corresponding to $d_i(6,8;2')$ and $d_s(2'';6,8)$ are unique among the dAs (Table I) serves as a further indication that the nucleotide dA_5 at the dA-dT junction is structurally unique among the nucleotides in this duplex. It is also worth mentioning that for all dTs the NOE cross-peaks corresponding to $d_i(6,8;2')$ are less intense than those for the dAs, which is against the trend expected from the values predicted from stereochemical considerations [Figure 11.6 in Wüthrich (1986)]. This implies that the values for the pseudorotation angle P and the glycosidic torsion angle χ for the dTs are different from those of the dAs and do not correspond to a standard C2′-endo conformation.

Both the inter- and intrastrand distances between A2H and 1′H (Figure 2, Table I) are too long for NOE observation in the "standard" B-DNA coordinates derived from Arnott's fiber diffraction data [Tables 11.2 and 11.4 in Wüthrich (1986)], but the variations of these distances between the individual nucleotides in single crystals of B-DNA extend to values that would be observable by NOESY [see Dickerson et al. (1985) and references cited therein]. Since there are too many degrees of freedom in the duplex, we cannot identify a unique structure that would be determined by the observation of these NOEs. Inspection of molecular models indicates that they would be compatible with distorted B-DNA forms, which include large propeller twisting for AT base pairs, as reported recently by Nelson et al. (1987) and Coll et al. (1987) from X-ray studies of oligonucleotides containing dA_n tracts.

(*c*) *Conclusions and Comparison with Literature Data.* The present experiments indicate that the B-DNA-type duplex d-(AAAAATTTTT)$_2$ contains a static distortion of the ring puckers of dT_6 and dT_7 away from a pure C2′-endo conformation. As a result there occurs a change of conformation at the dA_5-dT_6 junction within each of the two DNA strands. The deoxyribose ring puckers of dA and dT within the Watson–Crick base pairs A_5T_6 and A_4T_7 are therefore different. Combining the information from NOEs and from the analysis of the spin–spin coupling constants, we conclude that the deoxyribose conformation for dA_4 and dA_5 can be characterized by a value of the pseudorotation phase angle P in the range 150–180° and for dT_6 and dT_7 by a P value between 100 and 130°. Furthermore, the sequential and interstrand NOEs between adenine 2H and deoxyribose 1′H are compatible with pronounced propeller twisting of the AT base pairs.

With regard to the mechanism of DNA bending, it would be of interest to distinguish between the following two limiting structural situations: (i) All five nucleotides in the $(dA)_5$ tract or the $(dT)_5$ tract, respectively, would have identical local conformations, and a structural change would occur abruptly at the dA_5-dT_6 junction. (ii) The nucleotides dA_5 and dT_6 would have unique conformations, indicating that the structural transition extends from the dA_4-dA_5 junction to the dT_6-dT_7 junction. Unfortunately, the possibilities to distinguish between these two situations are somewhat limited. Thus, earlier work [e.g., Connolly and Eckstein (1984) and Otting et al. (1987)] had shown that the three terminal base pairs in DNA duplexes in solution are influenced by the proximity to the chain ends and should therefore be used only with great care for studies of sequence effects on the conformation. In d-(AAAAATTTTT)$_2$ the NMR data clearly demonstrate increased mobility of the deoxyribose ring in the 3′-terminal nucleotide, dT_{10}, whereas lack of sufficient spectral resolution of the deoxyribose protons prevented a detailed analysis for dT_8 and dT_9. For dA_1 to dA_3 the deviations of the NMR parameters from those expected for a pure C2′-endo conformation are again best explained by increased internal mobility of the deoxyribose ring, whereby the degree of mobility thus inferred is clearly smaller for the 5′-terminal dA than for the 3′-terminal dT. With regard to a distinction between the aforementioned structural situations i and ii, this means that we have to concentrate primarily on observations made with the central nucleotides dA_4 to dT_7, whereby one must also consider that dA_5 and dT_6 are in unique *sequence* locations. Data pointing toward a special structure for the central nucleotides dA_5 and dT_6 are that sequential NOEs corresponding to $d_s(2;1')$ are observed only between dA_4 and dA_5 and between dA_5 and dT_6, respectively (Table I), and that sequential NOEs between the methyl groups were observed for dT_7-dT_8 and dT_8-dT_9 but not for dT_6-dT_7. Also, the NOE corresponding to $d_i(1';4')$ is somewhat less intense for dT_7 than for dT_6 (Figure 3). Additional data that might have provided more information could not be collected because of the structural and spectroscopic equivalence of the two central base pairs, e.g., the interstrand NOE between the protons in position 2 of dA_5 (Patel et al., 1983). Overall, in view of the limited amount of data available, a predominance of either of the two aforementioned structures i or ii cannot be unambiguously established, but there are indications that the transition from the conformation seen for dA_4 to that of dT_7 extends over the central two nucleotides dA_5 and dT_6 rather than occurring as an abrupt change at the junctions dA_5-dT_6.

Several recent publications on oligonucleotide duplexes containing $(dA)_n$ tracts followed by one or several dTs are particularly interesting to compare with the results obtained here. The dodecanucleotide duplex d-(AAAAAATTTTTT)$_2$ (Roy et al., 1987) and the undecanucleotide duplex d-(CGAAAAATCGG)·d-(CCGATTTTTCG) (Kintanar et al., 1987) were studied in aqueous solution by NMR. For both compounds neither NOEs recorded at short mixing times nor data on spin–spin couplings have been reported as yet, and thus a detailed comparison of their structural properties with those of d-(AAAAATTTTT)$_2$ is not possible. However, there are qualitative spectral features that indicate that the conformations of the AT base pairs formed by the $(dA)_n$ tracts in these molecules are similar to those in the decanucleotide duplex d-(AAAAATTTTT)$_2$. This includes closely similar relative chemical shifts for the protons of the individual nucleotides near the dA-dT junction. Also, the interstrand A2H–1′H NOEs were stronger than the sequential ones, and as in d-(AAAAATTTTT)$_2$ all A2H–1′H NOEs are more intense than those in oligodeoxynucleotides containing only isolated AT base pairs (Behling & Kearns, 1986; Behling et al., 1987; Patel et al., 1986; Weiss et al., 1984b; even though the NOESY measurements in these references were all obtained with long mixing times, such a qualitative comparison should still be warranted). The similarity of these "fingerprints" for the different compounds appears to support the hypothesis that the variations in the deoxyribose ring puckers observed here for d-(AAAAATTTTT)$_2$ might be a general feature of duplexes containing $(dA)_n$ tracts followed by dT. It will be of interest to further investigate if and how variations in the deoxyribose ring conformations are related to bending of the DNA complex.

The crystal structures of d-(CGCAAAAAAGCG)·d-(CGCTTTTTTGCG) (Nelson et al., 1987) and d-$(CGCAAATTTGCG)_2$ (Coll et al., 1987) were found to exist in B-DNA-type global conformations. Again, at the resolution presented in these publications, a direct comparison with individual deoxyribose ring puckers is not possible. On the other hand, both structures contain pronounced propeller twists for the AT base pairs, which could be related to the A2H–1′H NOEs observed in solution and thus provide another indication that all the aforementioned $(dA)_n$-containing compounds might eventually be found to belong to the same conformational family.

All features of the IR spectrum of cast films of d-$(AAAAATTTTT)_2$ at high relative humidity (Taillendier et al., 1987) are in agreement with C2′-endo conformations for all deoxyriboses, whereas spectra taken of cast films at lower humidity exhibit additional features from C3′-endo sugar conformations. Thus, it would be interesting to run NMR spectra of aqueous d-$(AAAAATTTTT)_2$ under partially dehydrating conditions in order to obtain a more direct comparison with these IR data. The Raman spectra of aqueous d-$(AAAAATTTTT)_2$ solutions (Taillendier et al., 1987) are also in qualitative agreement with the results of the present NMR study. It should be mentioned that the higher proportion of sugars in C3′-endo conformations as deduced from Raman studies vs. NMR studies (20 ± 5% vs 8 ± 2%) might be due to the fact that the Raman marker band at 816 cm^{-1}, which was used for this estimation, was apparently erroneously assigned (Katahira et al., 1986). In a recent paper (Patapoff et al., 1988) microcrystals of d-$(AAAAATTTTT)_2$ were studied by polarized Raman spectroscopy. The conclusions were qualitatively the same as from the Raman study in aqueous solution (Taillendier et al., 1987). Specifically, the authors claim that by their method they are not able to detect that the decamer is appreciably bent in the crystal.

Acknowledgments

We are grateful to Drs. A. Klug and A. Rich and their colleagues for providing us with preprints on their work with single crystals of dA_n-containing DNA. We thank E. H. Hunziker-Kwik and R. Marani for the careful preparation of the figures and the manuscript.

Supplementary Material Available

Description of individual NMR experiments, assignments, and NMR spectra used and chemical shift table (10 pages). Ordering information is given on any current masthead page.

Registry No. d-(AAAAATTTTT), 85240-24-0.

References

Alexeev, D. G., Lipanov, A. A., & Skuratovskii, I. Ya. (1987a) *Nature 325*, 821–823.

Alexeev, D. G., Lipanov, A. A., & Skuratovskii, I. Ya. (1987b) *J. Biomol. Struct. Dyn. 4*, 989–1012.

Altona, C. (1982) *Recl. Trav. Chim. Pays-Bas 101*, 413–433.

Altona, C., & Sundaralingam, M. (1972) *J. Am. Chem. Soc. 94*, 8205–8212.

Altona, C., & Sundaralingam, M. (1973) *J. Am. Chem. Soc. 95*, 2333–2344.

Arnott, S., Chandrasekaran, R., Hall, I. H., & Puigjaner, L. C. (1983) *Nucleic Acids Res. 11*, 4141–4155.

Behling, R. W., & Kearns, D. R. (1986) *Biochemistry 25*, 3335–3346.

Behling, R. W., Rao, S. N., Kollman, P., & Kearns, D. R. (1987) *Biochemistry 26*, 4674–4681.

Benevides, J. M., Wang, A. H.-J., van der Marel, G. A., van Boom, J. H., & Thomas, G. J., Jr. (1988) *Biochemistry 27*, 931–938.

Celda, B., Leupin, W., & Wüthrich, K. (1986) *Abstracts of the I Reunión Española de Biofísica*, Sitges, Spain, Oct 1–4, p 42, Biophysical Society, Spain.

Challberg, S. S., & Englund, P. T. (1980) *J. Mol. Biol. 138*, 442–472.

Chary, K. V. R., Hosur, R. V., Girjesh Govil, Tan Zu-Kun, & Miles, H. T. (1987) *Biochemistry 26*, 1315–1322.

Chazin, W. J., Wüthrich, K., Rance, M., Hyberts, S., Denny, W. A., & Leupin, W. (1986) *J. Mol. Biol. 190*, 439–453.

Coll, M., Frederick, C. A., Wang, A. H.-J., & Rich, A. (1987) *Proc. Natl. Acad. Sci. U.S.A. 84*, 8385–8389.

Connolly, B. A., & Eckstein, F. (1984) *Biochemistry 23*, 5523–5527.

Davies, D. B. (1978) *Prog. Nucl. Magn. Reson. Spectrosc. 12*, 135–225.

Davies, D. B., & Danyluk, S. S. (1974) *Biochemistry 13*, 4417–4434.

Denny, W. A., Leupin, W., & Kearns, D. R. (1982) *Helv. Chim. Acta 65*, 2372–2393.

Dickerson, R. E., Kopka, M. L., & Pjura, Ph. (1985) in *Biological Macromolecules and Assemblies* (Jurnak, F. A., & McPherson, A., Eds.) Vol. 2, pp 37–126, Wiley, New York.

Edmondson, S. P. (1987) *Biopolymers 26*, 1941–1956.

Englund, P. T., Hajduk, S. L., & Marini, J. C. (1982) *Annu. Rev. Biochem. 51*, 695–726.

Feigon, J., Wright, J. M., Leupin, W., Denny, W. A., & Kearns, D. R. (1982) *J. Am. Chem. Soc. 104*, 5540–5541.

Feigon, J., Leupin, W., Denny, W. A., & Kearns, D. R. (1983) *Biochemistry 22*, 5943–5951.

Hagerman, P. J. (1984) *Proc. Natl. Acad. Sci. U.S.A. 81*, 4632–4636.

Hagerman, P. J. (1986) *Nature 321*, 449–450.

Hare, D. R., Wemmer, D. E., Chou, S.-H., Drobny, G., & Reid, B. R. (1983) *J. Mol. Biol. 171*, 319–336.

Hosur, R. V., Ravikumar, M., Chary, K. V. R., Anu Sheth, Girjesh Govil, Tan Zu-kun, & Miles, H. T. (1986) *FEBS Lett. 205*, 71–76.

Jollès, B., Laigle, A., Chinsky, L., & Turpin, P. Y. (1985) *Nucleic Acids Res. 13*, 2075–2085.

Katahira, M., Nishimura, Y., Tsuboi, M., Sato, T., Mitsui, Y., & Iitaka, Y. (1986) *Biochim. Biophys. Acta 867*, 256–267.

Kintanar, A., Klevit, R. E., & Reid, B. R. (1987) *Nucleic Acids Res. 15*, 5845–5862.

Koo, H.-S., & Crothers, D. M. (1987) *Biochemistry 26*, 3745–3748.

Koo, H.-S., Wu, H.-M., & Crothers, D. M. (1986) *Nature 320*, 501–506.

Levene, S. D., & Crothers, D. M. (1983) *J. Biomol. Struct. Dyn. 1*, 429–435.

Marini, J. C., Levene, S. D., Crothers, D. M., & Englund, P. T. (1982) *Proc. Natl. Acad. Sci. U.S.A. 79*, 7664–7668.

Nelson, H. C. M., Finch, J. T., Luisi, B. F., & Klug, A. (1987) *Nature 330*, 221–226.

Neuhaus, D., Wagner, G., Vašak, M., Kägi, J. H. R., & Wüthrich, K. (1985) *Eur. J. Biochem. 151*, 257–273.

Orbons, L. P. M., & Altona, C. (1986) *Eur. J. Biochem. 160*, 141–148.

Otting, G., Grütter, R., Leupin, W., Minganti, C., Ganesh, K. N., Sproat, B. S., Gait, M. J., & Wüthrich, K. (1987) *Eur. J. Biochem. 166*, 215–220.

Patapoff, T. W., Thomas, G. A., Wang, Y., & Peticolas, W. L. (1988) *Biopolymers 27*, 493–507.
Patel, D. J., Kozlowsky, S. A., & Ram Bhatt (1983) *Proc. Natl. Acad. Sci. U.S.A. 80*, 3908–3912.
Patel, D. J., Shapiro, L., & Hare, D. (1986) *J. Biol. Chem. 261*, 1223–1229.
Rance, M., Sørensen, O. W., Bodenhausen, G., Wagner, G., Ernst, R. R., & Wüthrich, K. (1983) *Biochem. Biophys. Res. Commun. 117*, 479–485.
Rhodes, D., & Klug, A. (1981) *Nature 292*, 378–380.
Rinkel, L. J., & Altona, C. (1987) *J. Biomol. Struct. Dyn. 4*, 621–649.
Roy, S., Borah, B., Zon, G., & Cohen, J. S. (1987) *Biopolymers 26*, 525–536.
Saenger, W. (1984) *Principles of Nucleic Acid Structure*, Springer, New York.
Sarma, M. H., Gupta, G., & Sarma, R. H. (1988) *Biochemistry 27*, 3423–3432.
Scheek, R. M., Russo, N., Boelens, R., Kaptein, R., & van Boom, J. H. (1983) *J. Am. Chem. Soc. 105*, 2914–2916.
Scheek, R. M., Boelens, R., Russo, N., van Boom, J. H., & Kaptein, R. (1984) *Biochemistry 23*, 1371–1376.
Simpson, L. (1979) *Proc. Natl. Acad. Sci. U.S.A. 76*, 1585–1588.
Taillendier, E., Ridoux, J.-P., Liquier, J., Leupin, W., Denny, W. A., Wang, Y., Thomas, G. A., & Peticolas, W. L. (1987) *Biochemistry 26*, 3361–3368.
Thomas, G. A., & Peticolas, W. L. (1983) *J. Am. Chem. Soc. 105*, 993–996.
Ti, G. S., Gaffney, B. L., & Jones, R. A. (1982) *J. Am. Chem. Soc. 104*, 1316–1319.
Travers, A. A., & Klug, A. (1987) *Philos. Trans. R. Soc. London, B 317*, 537–561.
Trifonov, E. N. (1986) *CRC Crit. Rev. Biochem. 19*, 89–106.
von Kitzing, E., & Diekmann, S. (1987) *Eur. Biophys. J. 15*, 13–26.
Weiss, M. A., Patel, D. J., Sauer, R. T., & Karplus, M. (1984a) *Proc. Natl. Acad. Sci. U.S.A. 81*, 130–134.
Weiss, M. A., Patel, D. J., Sauer, R. T., & Karplus, M. (1984b) *Nucleic Acids Res. 12*, 4035–4047.
Widmer, H. (1987) Ph.D. Thesis Nr.8369, ETH-Zürich.
Widmer, H., & Wüthrich, K. (1986) *J. Magn. Reson. 70*, 270–279.
Widmer, H., & Wüthrich, K. (1987) *J. Magn. Reson. 74*, 316–336.
Wu, H.-M., & Crothers, D. M. (1984) *Nature 308*, 509–513.
Wüthrich, K. (1986) *NMR of Proteins and Nucleic Acids*, Wiley, New York.
Zahn, K., & Blattner, F. R. (1985) *Nature 317*, 451–453.

Solid-Phase Synthesis and Side Reactions of Oligonucleotides Containing *O*-Alkylthymine Residues†

Henryk Borowy-Borowski and Robert W. Chambers*
Department of Biochemistry, Dalhousie University, Halifax, Nova Scotia B3H 4H7, Canada
Received July 18, 1988; Revised Manuscript Received September 14, 1988

ABSTRACT: As part of our studies on the molecular mechanism of mutation [Chambers, R. W. (1982) in *Molecular and Cellular Mechanisms of Mutagenesis* (Lemontt, J. F., & Generoso, W. M., Eds.) pp 121–145, Plenum, New York and London], we wanted to prepare specific oligonucleotides carrying O^2- or O^4-alkylthymidine residues. Since *O*-alkylthymine moieties are known to be alkali labile, side reactions were expected during the deprotection procedures used for synthesis of oligonucleotides on a solid support by the classical phosphoramidite method. We have studied these side reactions in detail. Kinetic data show the deprotection procedures displace most *O*-alkyl groups at rates that make these procedures inappropriate for synthesis of most oligonucleotides carrying *O*-alkylthymine moieties. We describe alternative deprotection procedures, using readily accessible reagents, that we have used successfully to synthesize a series of oligonucleotides carrying several different *O*-alkylthymine moieties. The oligonucleotides synthesized are d(A-A-A-A-G-T-alkT-T-A-A-A-A-C-A-T), where alk = O^2-methyl, O^2-isopropyl, O^4-methyl, O^4-isopropyl, and O^4-*n*-butyl. This work extends the previously described procedure for the chemical synthesis of oligonucleotides carrying an O^4-methylthymine moiety [Li, B. F., Reese, C. B., & Swann, P. F. (1987) *Biochemistry 26*, 1086–1093] and reports the first chemical synthesis of an oligonucleotide carrying an O^2-alkylthymine. The oligonucleotides synthesized have a sequence corresponding to the minus strand that is complementary to the viral strand at the start of gene G in bacteriophage ΦX174 replicative form DNA where the normal third codon has been replaced with the ocher codon, TAA.

When active carcinogens react with DNA, stable adducts form. Some of these adducts have been shown to produce mutations in vivo, and attention has focused on the possible role of these mutations in cancer. Using a combination of chemical and biochemical techniques, it is now possible to introduce these carcinogen–DNA adducts at preselected positions in biologically active DNA so that the mutagenic activity of the adduct and the effect that DNA repair has on that activity can be studied directly in living cells. The approach we have been using requires synthesis of an oligonucleotide having a predetermined sequence and carrying the

† This work was suspported by a Terry Fox Special Initiatives Award from the National Cancer Institute of Canada, by an operating grant from the Medical Research Council of Canada, and by an equipment grant from the Dalhousie Medical Research Fund.

0006-2960/89/0428-1471$01.50/0